Steel and Composite Structures, *Vol. 36, No. 5 (2020) 603-615*
DOI: https://doi.org/10.12989/scs.2020.36.5.603

Runge-Kutta method for flow of dusty fluid along exponentially stretching cylinder

Waheed Iqbal[1], Mudassar Jalil[2], Mohamed A. Khadimallah[3], Hamdi Ayed[4,5], Muhammad N. Naeem[1], Muzamal Hussain*[1], Souhail Mohamed Bouzgarrou[6], S.R. Mahmoud[7], E. Ghandourah[8], Muhammad Taj[9] and Abdelouahed Tounsi[10,11]

[1]*Department of Mathematics, Govt. College University Faisalabad, 38000, Faisalabad, Pakistan*
[2]*Department of Mathematics, COMSATS Institute of Information Technology, Park Road, Chak Shahzad, 44000 Islamabad, Pakistan*
[3]*Prince Sattam Bin Abdulaziz University, College of Engineering, Civil Engineering Department, BP 655, Al-Kharj, 11942, Saudi Arabia*
[4]*Department of Civil Engineering, College of Engineering, King Khalid University, Abha, Kingdom of Saudi Arabia*
[5]*Higher Institute of Transport and Logistics of Sousse, University Sousse, Tunisia*
[6] *Department of Civil Engineering, Faculty of Engineering, Jazan University, Kingdom of Saudi Arabia*
[7]*GRC Department, Faculty of Applied studies, King Abdulaziz University, Jeddah, Saudi Arabia*
[8]*Department of Nuclear Engineering, Faculty of Engineering, King Abdulaziz University, Jeddah, Saudi Arabia*
[9]*Department of Mathematics, University of Azad Jammu and Kashmir, Muzaffarabad, 1300, Azad Kashmir, Pakistan*
[10]*Department of Technology Civil Engineering, Materials and Hydrology Laboratory, University of Sidi Bel Abbes, Algeria*
[11]*Department of Civil and Environmental Engineering, King Fahd University of Petroleum & Minerals, 31261 Dhahran, Eastern Province, Saudi Arabia*

(*Received May 25, 2020, Revised August 7, 2020, Accepted August 11, 2020*)

Abstract. The present manuscript focuses on the flow and heat transfer of the dusty fluid along exponentially stretching cylinder. Enormous attempts are made for fluid flow along cylinder but the study of fluid behavior along exponentially stretching cylinder is discussed lately. Using appropriate transformations, the governing partial differential equations are converted to non-dimensional ordinary differential equations. The transformed equations are solved numerically using Shooting technique with Runge-Kutta method. The influence of the physical parameters on the velocity and temperature profiles as well as the skin fraction coefficient and the local Nusselt number are examined in detail. The essential observations are as the fluid velocity decreases but temperature grows with rise in particle interaction parameter, and both the fluid velocity and temperature fall with increase in mass concentration parameter, Reynold number, Particle interaction parameter for temperature and the Prandtl number.

Keywords: dusty fluid; stretching cylinder; exponential stretching; shooting method; numerical solution

1. Introduction

Fluid flow behavior along the stretching cylinder in various physical conditions has gained considerable attention over the past few decades. Reasons behind the great interest are its several implementations in many advance industrial techniques such as composite processing, gas cooling systems, processing of plastic foam, polymer technology, watering system channels, cement process industry and many more. Firstly, Wang 1988 studied the fluid behavior along the stretching cylinder. The detailed study of fluid flow along the stretched cylinder for the boundary layer was made (Ishak and Nazar 2009) regarding. Wang (2011) obtained asymptotic solutions for high Reynold number using slip flow condition. Mixed convection condition together with slip flow and obtained numerical solution for the boundary layer problem of Williamson fluid flow over a stretching cylinder (Salahuddin *et al*. 2017). The effects of Soret and Dufour for the Casson fluid by considering the heat transfer along stretching cylinder was worked out (Mahdy 2015). The mass and convective heat conditions for Casson fluid flow having nanoparticles along stretching cylinder was presented (Maria *et al*. 2016). A thorough numerical study of sisko fluid flow over stretching cylinder with effects of thermal conductivity and viscous dissipation was done (Malik *et al.*2016). Al-Maliki et al. (2020) carried out the dynamic analysis of functionally graded (FG) graphene-reinforced beams under thermal loading based on finite element approach. The presented formulation is based on a higher order refined beam element accounting for shear deformations. The graphene-reinforced beam is exposed to transverse periodic mechanical loading.

The uniform suction/blowing effects together with transfer of heat outside the permeable stretching cylinder were considered (Ishaq *et al*. 2008). Under convective boundary conditions, electrically conducting sisko fluid along the stretching cylinder in axial direction was probed (Khan and Malik 2015). They found the considerable boost in the flow parameters for shear thinning than thickening. The notable point about all the above mentioned studies is

∗Corresponding author, Ph.D.
E-mail: muzamalhussain@gcuf.edu.pk

http://www.techno-press.org/?journal=scs&subpage=8
ISSN: 1229-9367 (Print), 1598-6233 (Online)

that the considered fluid is "Pure". Practically it is almost impossible to have such fluid which is free from any kind of impurity. Every naturally occurring fluid contains dust particles. Many engineering and industrial problems deal with dusty fluid such as powder mechanization and centrifugal technique to the detachment of particles from the fluid. Flow of dusty fluid can be viewed in many natural phenomena e.g., flow of mud in rivers, blood flow and atmospheric flow during haze. Initiative study of motion of dust particles in laminar flow has been carried out (Saffman, 1962). An analysis for viscous, incompressible steady flow of dusty fluid flowing between two co-axial rotating cylinders under pressure gradient effect was carried out (Girishwar 1970). Akgoz and Civalek (2011) investigated geometrically the nonlinear free vibration analysis of thin laminated plates resting on non-linear elastic foundations. Winkler-Pasternak type foundation model is used. Governing equations of motions are obtained using the von Karman type nonlinear theory. The method of discrete singular convolution is used to obtain the discretised equations of motion of plates. Sharma *et al.* (2018e) presented the novel higher-order coupled finite-boundary element scheme for the computation of the thermoacoustic responses of the layered panel structure under the harmonic excitation. The thermally pre-stressed vibrating composite panel model is derived mathematically using the higher-order shear deformation mid-plane kinematics. Batou *et al.* (2019) studied the wave propagations in sigmoid functionally graded (S-FG) plates using new Higher Shear Deformation Theory (HSDT) based on two-dimensional (2D) elasticity theory. The current higher order theory has only four unknowns, which mean that few numbers of unknowns, compared with first shear deformations and others higher shear deformations theories and without needing shear corrector.

Baaskaran *et al.* (2018) studied the reliable and accurate method of computationally aided design processes of advanced thin walled structures in automotive industries for the efficient usage of smart materials, that possess higher energy absorption in dynamic compression loading. The most versatile components ie, thin walled crash tubes with different geometrical profiles are introduced in view of mitigating the impact of varying cross section in crash behavior and energy absorption characteristics. Sharma *et al.* (2018c, d) carried out numerically the acoustic radiation responses of doubly curved laminated composite shell panels subjected to harmonic excitation are investigated numerically in the framework of the higher-order shear deformation theory. A general mathematical model for the vibrating curved panel has been developed and the cylindrical, spherical, elliptical and hyperboloid shell panel geometries resting on an infinite rigid baffle are considered for analysis. A numerical scheme for the vibrating plate has been developed in the frame work of the higher-order mid-plane kinematics and the eigen frequencies are obtained by employing suitable finite element steps. Dusty gas flow in a region occupied by boundary layer was examined (Chakrabarti 1974). The coefficient of friction and heat transfer for dusty boundary layer flow with pressure gradient was studied (Agranat 1988). In addition to these studies for flow and transfer of heat for dusty fluid along sheet / surface, many researchers considered dusty fluid flow along cylinder. The viscous, incompressible gas flow having dust particles for an isothermal cylinder was discussed and results from various physical parameters were presented (Rebhi 2010). Chen *et al.* (2019a, b) carried the energy absorption characteristics of a lattice-web reinforced composite sandwich cylinder (LRCSC) which is composed of glass fiber reinforced polymer (GFRP) face sheets, GFRP lattice webs, polyurethane (PU) foam and ceramsite filler. The vortex-induced vibration of three circular cylinders (each of diameter D) in an equilateral triangular arrangement is investigated using the immersed boundary method. Abdulrazzaq *et al.* (2020) investigated the thermo-elastic buckling of small scale functionally graded material (FGM) nano-size plates with clamped edge conditions rested on an elastic substrate exposed to uniformly, linearly and non-linearly temperature distributions employing a secant function based refined theory. Material properties of the FGM nano-size plate have exponential gradation across the plate thickness. Civalek (2017) investigated the free vibration analysis of conical and cylindrical shells and annular plates made of composite laminated and functionally graded materials (FGMs). Carbon nanotubes reinforced (CNTR) composite case is also taken consideration for FGM. The equations of motion for conical shell are obtained via Hamilton's principle using the transverse shear deformation theory. Sharma *et al.* (2018a, b) studied the vibroacoustic responses of laminated composite curved panels subjected to harmonic point excitation in a combined temperature and moisture environment using a novel higher-order finite-boundary element model. The hygrothermal dependent composite material properties are incorporated macroscopically in the formulation. The natural frequencies alongside corresponding modes of the flat panels resting on an infinite rigid baffle are obtained by using finite element method in the framework of the higher-order shear deformation theory. Some valuable results regarding heat transfer of dusty fluid over a hollow stretching cylinder using multi-step DTM were reported (Rasekh *et al.* 2013). Conduction of dusty fluid flow along stretching cylinder with thermal conductivity and viscosity effects were dealt numerically (Konch and Hazarika 2017). Derakhshandeh1a *et al.* (2020) investigated the Reynolds number Re (= 50-200) effects on the flows around a single cylinder and the two tandem (center-to-center spacing $L*= L/D= 4$) cylinders, each of a diameter D. Vorticity structures, Strouhal numbers, and time-mean and fluctuating forces are presented and discussed. Sharma *et al.* (2017 a, b, c) investigated the vibro-acoustic responses of the laminated composite flat panel in an infinite rigid baffle under the influence of central and eccentric harmonic point excitation. A general mathematical model of the flat panel is developed in the framework of the higher order shear deformation theory to compute the vibrational properties. The frequency values of the panel are obtained by using simulation model through the commercial finite element package (ANSYS) via batch input technique. he structural responses are obtained using a

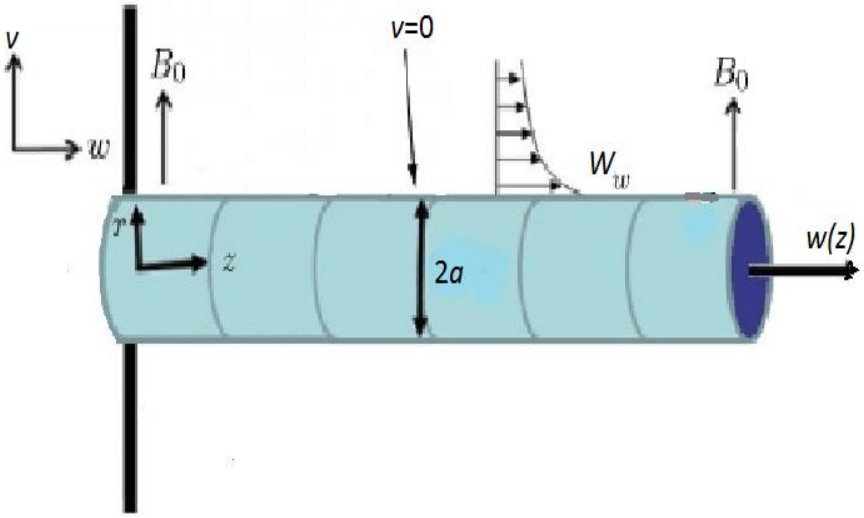

Fig. 1 The geometry of the cylinder

simulation model via ANSYS including the effect various geometries (cylindrical, elliptical, spherical and hyperboloid). Initially, the model has been established by solving adequate number of available examples to show the convergence and comparison behaviour of the natural frequencies. Salah *et al.* (2019) employed a simple four-variable integral plate theory for examining the thermal buckling properties of functionally graded material (FGM) sandwich plates. The proposed kinematics considers integral terms which include the effect of transverse shear deformations. In some fresh attempts, the researchers have pondered over new dimensions of stretching i.e., exponentially stretching cylinder. The detailed study of flow and transfer of heat for hyperbolic tangent fluid over a stretching cylinder exponentially in vertical direction was carried out (Naseer *et al.* 2014). Shadravan *et al.* (2019) performed lateral load testing on seventeen wood wall frames in two sections. Section one included eight tests studying structural foam sheathing of shear walls subjected to monotonic loads following the ASTM E564 test method.

Similarity solution has been derived for steady boundary layer and heat flow of Casson nanofluid (Malik *et al.* 2013) while cylinder was stretching exponentially along its radius. The flow of Micropolar fluid through vertical exponentially stretching cylinder along the axial direction and discussed heat transfer effects, too, were considered (Rehman *et al.* 2015). Williamson fluid flow along an exponentially stretching cylinder was examined and they found its numerical solution (Iqbal *et al.* 2018). Recently some researcher used different methods for nonlinear modeling (Avcar 2019, Karami *et al.* 2017, 2018, Madani *et al.* 2016, Simsek 2011).

Open see softare (Moghaddam and Masoodi 2019), first order shear deformation theory (Loghman *et al.* 2018), MLPG method (Rad *et al.* 2020), Ritz-type variational method (Sofiyev *et al*. 2006), Multiphysical numerical (FE–BE) solution and higher-order shear theory (Sharma *et al.* 2019a, b, 2020 a, b).

The foremost intension of present study is to investigate the importance of dusty fluid flow in the field of fluid dynamics and the research in new dimension of stretching cylinder using Runge-Kutta method, which is our particular motivation. Many material researchers used different methodologies to investigate the structure of computational mechanics as: open see softare (Moghaddam and Masoodi, 2019), first order shear deformation theory (Loghman *et al.* 2018), MLPG method (Rad *et al.* 2020), Ritz-type variational method (Sofiyev *et al.* 2006), multiphysical numerical (FE–BE) solution and higher-order shear theory (Sharma *et al.* 2019a, b, 2020 a, b). The suggested method to investigate the flow and heat transfer effects of a dusty fluid along exponentially stretching cylinder is Runge-Kutta method, which is a well-known and efficient technique to develop the fundamental frequency equations. This method converge fastly than other methods. It is keenly seen from the literature, no evidence is found concerning current model. The transformed equations are solved numerically using Shooting technique with Runge-Kutta method. The influence of the physical parameters on the velocity and temperature profiles as well as the skin fraction coefficient and the local Nusselt number are examined in detail. The essential observations are as the fluid velocity decreases but temperature grows with rise in particle interaction parameter, and both the fluid velocity and temperature fall with increase in mass concentration parameter, Reynold number, Particle interaction parameter for temperature and the Prandtl number.

2. Methodology

Consider laminar, steady, incompressible boundary layer flow of dusty viscous fluid in two dimensions along a hollow cylinder. The cylinder is stretching exponentially along positive z-axis with velocity $U_w = 2ace^{z/a}$, where c is the stretching rate. The origin of stationary cylindrical coordinate system has been positioned in the middle of the cylinder's leading edge, the z-axis is taken along the axis of the cylinder and the r-axis is assumed in the direction of radius of cylinder as shown in Fig. 1.

The flow of dust fluid is controlled by stretching of the cylinder and the surface temperature $T_w = T_\infty + Ae^{(z/a)}$. Both the dust particles and the fluid are taken initially to be in fixed position. We assume that particles of dust are in spherical form, having uniform size and constant number density. Under these suppositions along the Boussinesq and the boundary layer approximation the governing equations for the flow behavior are

$$\frac{\partial(rw)}{\partial z}+\frac{\partial(ru)}{\partial r}=0, \tag{1}$$

$$w\frac{\partial w}{\partial z}+u\frac{\partial w}{\partial r}=\nu\left(\frac{\partial^2 w}{\partial r^2}+\frac{1}{r}\frac{\partial w}{\partial r}\right)+\frac{\gamma}{\tau_v}\left(w_p-w\right) \tag{2}$$

$$w_p\frac{\partial w_p}{\partial z}+u_p\frac{\partial w_p}{\partial r}=\frac{1}{\tau_v}\left(w-w_p\right) \tag{3}$$

$$\frac{\partial(rw_p)}{\partial z}+\frac{\partial(ru_p)}{\partial r}=0, \tag{4}$$

$$\begin{aligned}&w\frac{\partial T}{\partial z}+u\frac{\partial T}{\partial r}=\alpha\left(\frac{\partial^2 T}{\partial r^2}+\frac{1}{r}\frac{\partial T}{\partial r}\right)+\\&\frac{\gamma}{\tau_T}\left(T_p-T\right)+\frac{\gamma}{c_p\tau_v}\left(w_p-w\right)^2\end{aligned} \tag{5}$$

$$w_p\frac{\partial T_p}{\partial z}+u_p\frac{\partial T_p}{\partial r}=\frac{c_p}{c_m\tau_T}\left(T-T_p\right) \tag{6}$$

The components of velocity and temperature of fluid and the dust particles are (u,w,T) and (u_p,w_p,T_p) respectively in (r,z) directions. Parameter $\gamma(=\frac{mN}{\rho})$ denotes the mass concentration of dust particles, $\tau_v=\frac{m}{K}$, is the relaxation time of particle phase and τ_T, represents the thermal equilibrium time, here ρ, ν and α are density, kinematic viscosity and thermal diffusivity of the fluid, respectively. Dusty fluid parameters K, N and m are the Stoke' s resistance, number density and mass concentration of dust particle. Specific heat parameters of fluid and dust particles are denoted by c_p and c_m, respectively. The boundary conditions related to above system are

$$\begin{aligned}&r=a; \quad w=U_w,\ u=0,\ T=T_w=T_\infty+Ae^{(z/a)}\\&r\to\infty; \quad w=0,\ w_p=0,\ u_p=u,\\&\quad T\to T_\infty,\ T_p\to T_\infty.\end{aligned} \tag{7}$$

Eqs. (1) and (6) are non-linear coupled PDEs. These equations can easily be transformed into set of ODEs by using similarity transformations.

$$\begin{aligned}&\zeta=\left(\frac{r}{a}\right)^2,\ u=-\frac{1}{2}U_w\frac{g(\zeta)}{\sqrt{\zeta}},\\&w=U_w g'(\zeta),\ \theta(\zeta)=\frac{T-T_\infty}{T_w-T_\infty},\\&u_p=-\frac{1}{2}U_w\frac{h(\zeta)}{\sqrt{\zeta}},\\&w_p=U_w h'(\zeta),\ \theta_p(\zeta)=\frac{T_p-T_\infty}{T_w-T_\infty},\end{aligned} \tag{8}$$

The differentiation w.r.t ζ is represented by prime. By employing the above similarity transformation Eqs. (1) and (4) are identically satisfied and other equations are transformed to

$$\zeta g'''+g''+\mathrm{Re}\left(gg''-g'^2\right)+\beta_v\gamma\left(h'-g'\right)=0, \tag{9}$$

$$\mathrm{Re}\left(hh''-h'^2\right)+\beta_v\left(g'-h'\right)=0, \tag{10}$$

$$\begin{aligned}&\zeta\theta''+\theta'+\mathrm{Pr}\,\mathrm{Re}\left(g\theta'-g'\theta\right)+\mathrm{Pr}\,\gamma\,\beta_T\left(\theta_p-\theta\right)\\&+\mathrm{Pr}\,\gamma\,\beta_v Ec\left(h'-g'\right)^2=0,\end{aligned} \tag{11}$$

$$\mathrm{Re}\left(h'\theta_p-h\theta_p'\right)+\delta\beta_T\left(\theta_p-\theta\right)=0, \tag{12}$$

Where the non-dimensional parameters $\mathrm{Re},\beta_v,\gamma,\beta_T,\mathrm{Pr},Ec,\beta_T,\delta$ and δ are defined as

$$\begin{aligned}&\beta_v=\frac{a^2}{4\nu\tau_v},\gamma=\frac{mN}{\rho},\mathrm{Re}=\frac{aU_w}{4\nu},\\&Ec=\frac{U_w{}^2}{c_p(T_w-T_\infty)},\mathrm{Pr}=\frac{\nu}{\alpha},\beta_T=\frac{a^2}{4\nu\tau_T},\delta=\frac{c_p}{c_m},\end{aligned} \tag{13}$$

Here, β_v is fluid particle interaction parameter, γ is mass concentration parameter, Re is the Reynold number, Ec is the Eckert number, Pr is the Prandtl number, β_T is the fluid-particle interaction parameter for temperature and δ is the specific ratio, respectively. The transformed boundary conditions are

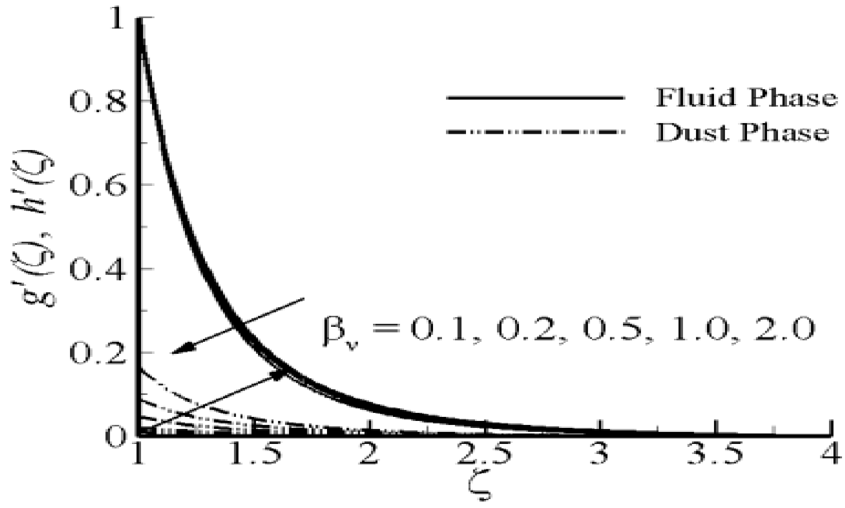

Fig. 2 Impact of particle interaction parameter on profile of velocity

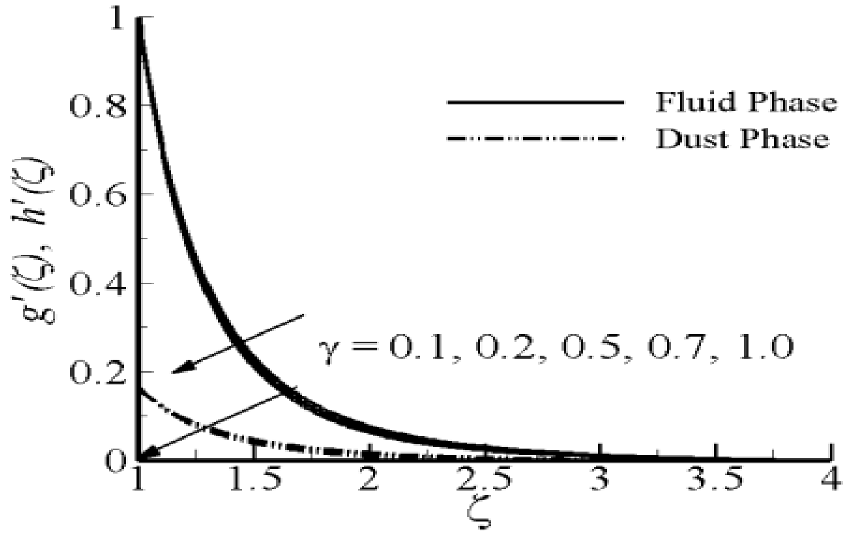

Fig. 3 Impact of mass concentration parameter on profile of velocity

$$
\begin{aligned}
&g(1)=0,\ g'(1)=1,\ g'(\infty)=0,\ \theta(1)=1.\\
&h'(\zeta)=0,\ h(\zeta)=g(\zeta),\ \theta(\zeta)=0,\\
&\theta_p(\zeta)=0\ \ as\ \zeta\to\infty.
\end{aligned}
\tag{14}
$$

The skin friction coefficient C_f and the Nusselt number Nu are defined as

$$C_f=\frac{\tau_w}{\rho U_w^{\,2}/2}, \tag{15}$$

$$Nu=\frac{aq_w}{k(T_w-T_\infty)}, \tag{16}$$

where τ_w and q_w are the shear stress and rate of heat transfer, respectively. These quantities are defined by

$$\tau_w=\mu\left(\frac{\partial w}{\partial r}\right)\bigg|_{r=a}, \tag{17}$$

$$q_w=-k\left(\frac{\partial T}{\partial r}\right)\bigg|_{r=a}, \tag{18}$$

Using the similarity transformation (8) in Eqs. (17) and (18) and substituting it in Eqs. (15) and (16), the dimensionless skin friction coefficient and Nusselt number are achieved like

$$C_f\,\mathrm{Re}=g^{n}(1) \tag{19}$$

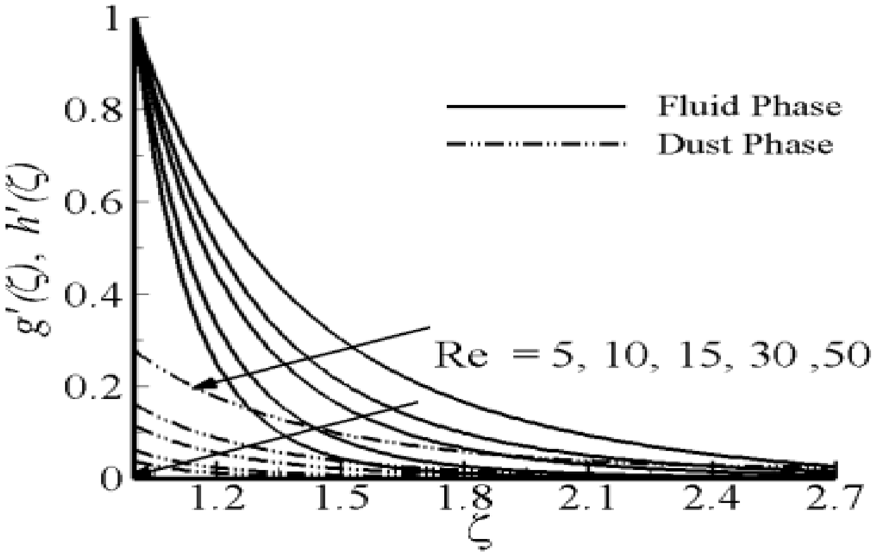

Fig. 4 Impact of Reynold number on profile of velocity

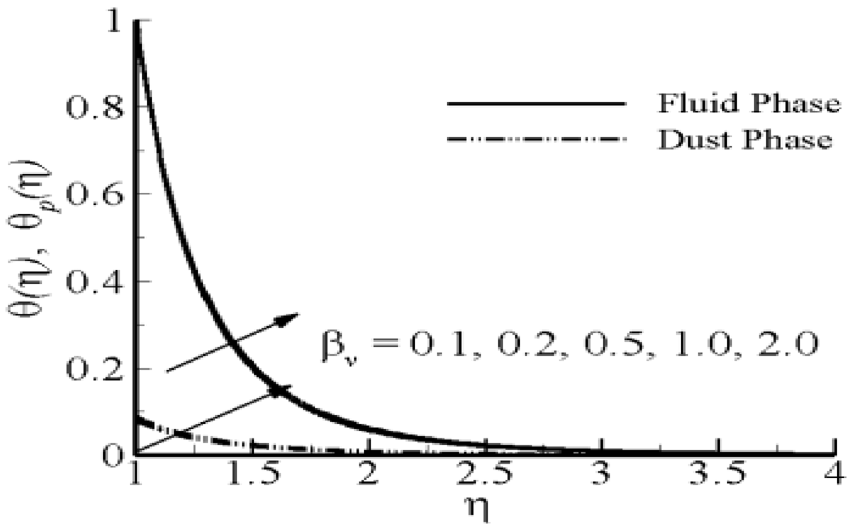

Fig. 5 Impact of particle interaction parameter on profile of temperature

$$Nu/2 = -\theta'(1) \tag{20}$$

Eqs. (9) - (12) are non-linear coupled ODEs. Exact analytical solution of above equations are not possible, therefore in the coming section numerical results of the problem are discussed and presented.

3. Results and discussion

Numerical solution of Eqs. (9) - (12) along with boundary condition (14) is attained through shooting method with RK-6. Consequences of the impact of particle interaction parameter β_v, the mass concentration parameter γ and the local Reynold number *Re* over the velocity profile of fluid and dust phase are elaborated with graphical Figs. 2-4 while Figs. 5-11 show the variation of particle interaction parameter β_v, the mass concentration parameter γ, local Reynold number *Re*, particle interaction parameter for temperature β_T, the Eckert number *Ec*, the prandtl number *Pr* and the specific ratio δ over the temperature profile.

Fig. 2 represents the profile of the velocity for various non-identical values of the particle interaction parameter for phases of fluid and dust. It is seen in the graph that velocity of dust phases increases for large values of particle

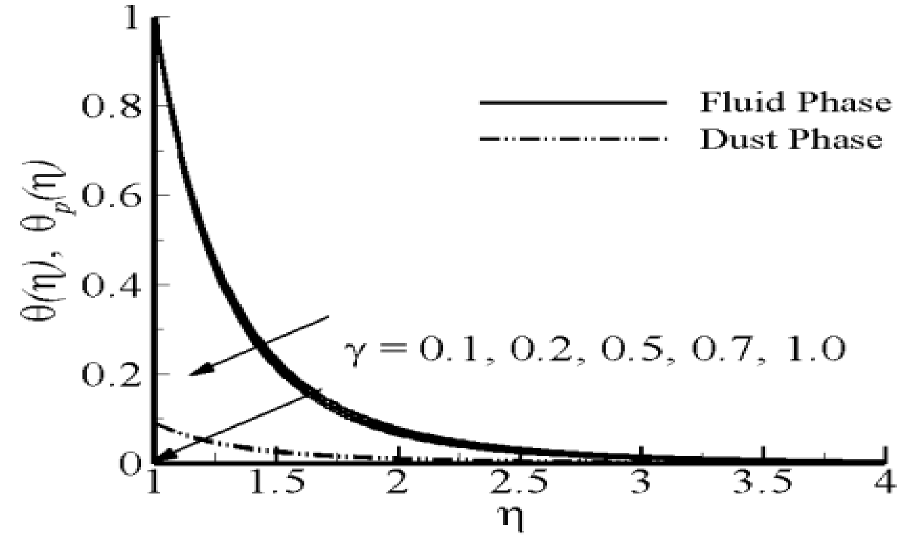

Fig. 6 Impact of mass concentration parameter on profile of temperature

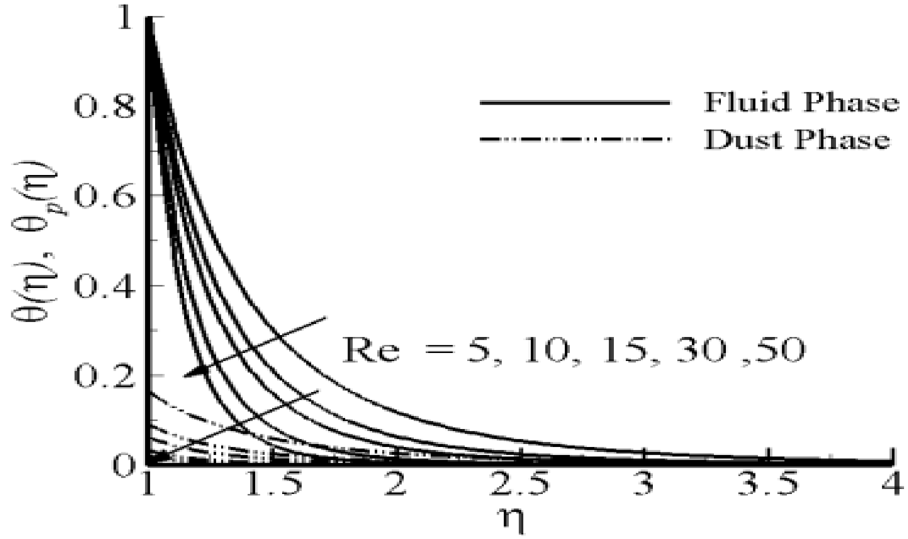

Fig. 7 Impact of Reynold number on profile of temperature

interaction parameter while there is fall in velocity for fluid phase. In fact, by increasing the fluid-particle interaction parameter the fluid and dust particles interaction also increases so the dust phase velocity enhances until the relative velocity of the fluid and particle phase become identical. On the other hand, increasing the fluid-particle interaction parameter the suspension of dust particles is increased that produces an internal friction within the fluid as a result the fluid phase velocity decreases. In Fig. 3, it is clearly shown that velocity decreases for both the fluid and dust phases on increasing the mass concentration parameter. The reason is that; more mass concentration will result in increase in viscosity which ultimately reduces the velocity.

While in Fig. 4, impact of local Reynold number (*Re*) on profile of the velocity of both dust and fluid phases is shown graphically. It is obvious from the figure that by increasing the Reynold number (*Re*) viscous forces dominates, and velocity decreases in both the phases. In Figs. 2-4 the values of parameters are taken as $\beta_v = 2$, $\gamma = 1$ & $Re = 10$. The variation of skin friction coefficient $-g''(1)$ with local Reynold number *Re*, particle interaction parameters β_v and the mass concentration parameter γ has been tabulated in Table 1. It is evident that skin friction coefficient is found to increase for increasing values of *Re*, βv and γ. Because, rise in *Re* increases viscous forces which ultimately increases skin friction coefficient, similarly increasing dusty fluid parameters produces higher resistance

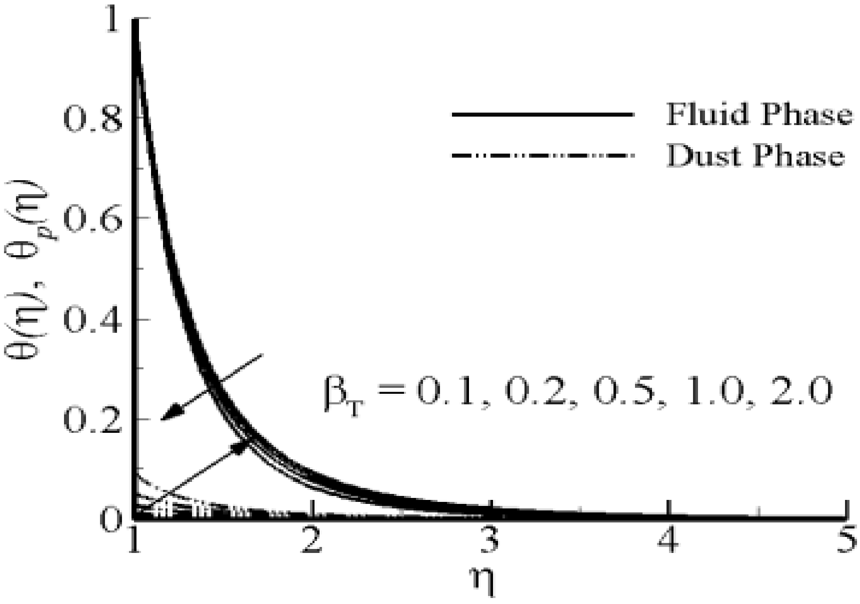

Fig. 8 Impact of particle interaction parameter of temperature on profile of temperature

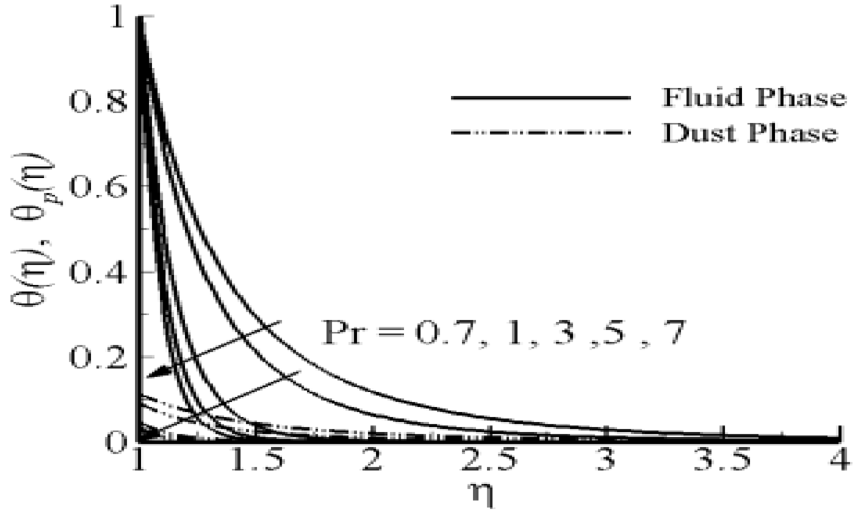

Fig. 9 Impact of Prandtl number on profile of temperature

to the flow and then skin friction is also increased. Fig. 5, depicts the impact of particle interaction parameter on temperature profile. A noticeable increase is observed in temperature for higher values of β_v. Here collision rate goes up and in turns kinetic energy (K.E) increases. K.E has direct relation to the temperature. So, increase in particle interaction results in high temperature for both the fluid and the dust phases. Fig. 6 gives a graphical picture of variation in mass concentration parameter over temperature profile. Higher values of γ, results in more number of dust particles which in turns slow down the velocity. So, ultimate result is reduction in heat transfer rate for both the phases of fluid. Decrease in temperature profile is noted in Fig. 7 for increasing values of *Re* for both the phases. As *Re* is in inverse relation with viscosity, there is a decrease in friction factor which produces depreciation in temperature. Growing values of particle interaction parameter give rise in the velocity of the dust and fluid particles until both acquire the same velocity, then more collision enhances the temperature of the dust phase. But at this moment, another prominent change occur i.e., increase in suspension of dust particles which slows down the fluid so finally temperature drops for the fluid phase as depicted in Fig. 8. Behavior of Prandtl number on profile of temperature is shown in Fig. 9. In physical sense, Prandtl number has inverse relation with thermal diffusivity, so weak diffusion of heat energy is

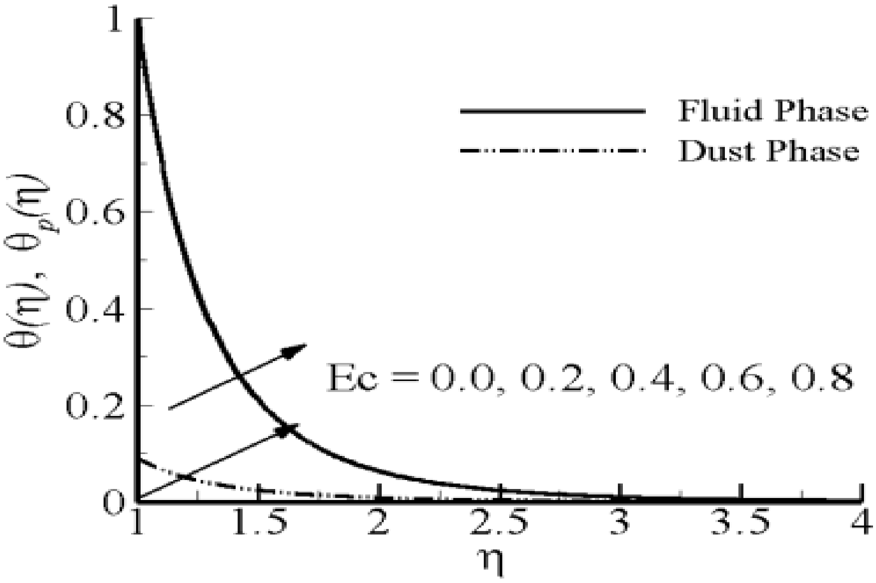

Fig. 10 Impact of Eckert number on profile of temperature

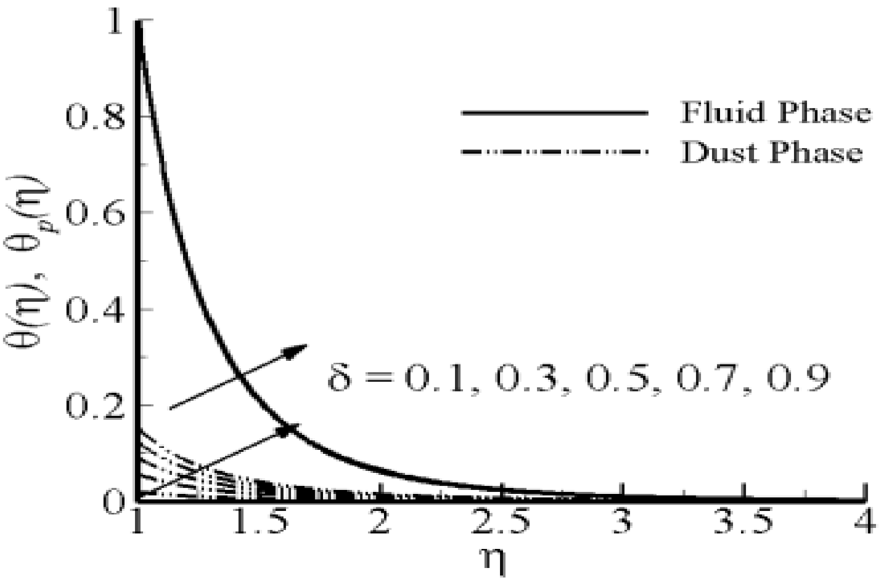

Fig. 11 Impact of specific ratio on profile of temperature

observed for ascending *Pr*, which consequently lowers down the temperature. Fig. 10 response of Eckert number on profile of temperature is exhibited. Temperature goes up for both the dust and the fluid phases by increasing the *Ec*. It can be justified by keeping in view that *Ec* enhances bouncy forces in the fluid which increase the collision of particles. Through collision more energy is accumulated in fluid and temperature is raised. Specific ratio is the required heat energy to raise unit temperature of unit substance. It means at high specific ratio more heat energy is provided, logically temperature goes high for both the dust and the fluid phases as shown in Fig. 11. In Table 2 (a) and (b), Nusselt number decreases for larger values of $\mathrm{Re}, \gamma, \beta_T$ and Pr, while inverse behavior is observed for β_v, Ec and δ. Such behavior is justified as Nesselt number goes high with increasing temperature. Ultimately convictive heat transfer occurs with rising temperature. Same trend has been followed in case β_v, Ec and δ where notable increase in Nesselt number is seen. While inverse mood of $\mathrm{Re}, \gamma, \beta_T$ and Pr is observed due to the same reason.

Table 1 For different values of Re, β_v and γ numerical value of $g''(1)$

Re	β_v	γ	$-g''(1)$
5	2	1	2.741649
10			3.612068
15			4.287201
30			5.834313
50			7.392431
10	0.1		3.364133
	0.2		3.379972
	0.5		3.425116
	1		3.493254
	2		3.612082
		0.1	3.374806
		0.2	3.401936
		0.5	3.481566
		0.7	3.533639
		1.0	3.612082

Table 2a For various values of $\mathrm{Re}, \beta_v, \gamma, \beta_T, \mathrm{Pr}, Ec$ and δ numerical values of $-\theta'(1)$

Re	β_v	γ	β_T	Pr	Ec	δ	$-\theta'(1)$
5	2	1	2	1	0.5	0.5	2.718925
10							3.564225
15							4.234356
30							5.784181
50							7.348750
10	0.1						3.687892
	0.2						3.678863
	0.5						3.653923
	1						3.618422
	2						3.564225
		0.1					3.367754
		0.2					3.390304
		0.5					3.456823
		0.7					3.500279
		1.0					3.564225

4. Conclusions

The laminar boundary layer flow behavior and heat transfer of dusty viscous fluid in two dimensions subject to the steady, incompressible conditions has been studied numerically. The impact of different physical parameters on velocity and temperature profile is discussed and shown graphically.

Some significant points are as follows: -

1. An increase in velocity is noted for dust phase while there is a decrease in the phase of fluid for the impact of particle interaction parameter β_v.

2. A considerable rise in the velocity profile for both the dust and fluid phases is seen with the impact of mass concentration parameter γ.

3. For local Reynold number Re effect a notable decrease in velocity for dust and fluid phases is observed.

4. All the parameters i.e., particle interaction β_v, mass concentration γ & Reynold number (Re) enhance skin friction coefficient.

Table 2b For various values of $\mathrm{Re}, \beta_v, \gamma, \beta_T, \mathrm{Pr}, Ec$ and δ numerical values of $-\theta'(1)$

Re	β_v	γ	β_T	Pr	Ec	δ	$-\theta'(1)$
10	2	1	0.1	1	0.5	0.5	3.218158
			0.2				3.240484
			0.5				3.303769
			1				3.399314
			2				3.564225
				0.7			2.903240
				1			3.564225
				3			6.537192
				5			8.574081
				7			10.224347
					0		3.637020
					0.2		3.607902
					0.4		3.578784
					0.6		3.549666
					0.8		3.520548
						0.1	3.593417
						0.3	3.578280
						0.5	3.564225
						0.7	3.551147
						0.9	3.538953

5. Temperature of the fluid increases for both the phases for ascending values of particle interaction parameter (β_v).

6. Reduction of temperature is reported for the larger values of mass concentration parameter (γ).

7. Increase in Reynold number (Re) results in fall of temperature.

8. Larger values of particle interaction parameter for temperature (β_T) boost up the temperature of dust phase while decreases for the fluid phase.

9. Decline in temperature is noted for high values of Prantl number (Pr).

10. Temperature increases with the increase of Eckert number (Ec).

11. Impact of increasing specific ratio (δ) is also in ascending order for temperature.

12. Local Nusselt number increases with parameter β_v, Ec *and* δ whereas showing opposite relation in case of $\mathrm{Re}, \gamma, \beta_T$ and Pr ..

Declaration of Conflicting Interests

The author(s) declared no potential conflicts of interest with respect to the research, authorship, and/or publication of this article.

Funding

The author(s) received no financial support for the research, authorship, and/or publication of this article.

ORCID iD

Muzamal Hussain http://orcid.org/0000-0002-6226-359X.

References

Abdulrazzaq, M.A., Fenjan, R.M., Ahmed, R.A. and Faleh, N.M. (2020), "Thermal buckling of nonlocal clamped exponentially graded plate according to a secant function based refined theory", *Steel Compos. Struct.*, **35**(1), 147-157. https://doi.org/10.12989/scs.2020.35.1.147.

Agranat, V.M. (1988), Effect of pressure gradient on friction and heat transfer in a dusty boundary layer", *Fluid Dyn.*, **23**, 729-732. http://dx.doi.org/10.1007/BF02614150.

Akgoz, B. and Civalek, O. (2011), "Nonlinear vibration analysis of laminated plates resting on nonlinear two-parameters elastic foundations", *Steel Compos. Struct.*, **11**(5), 403-421 https://doi.org/10.12989/scs.2011.11.5.403.

Al-Maliki, A.F., Ahmed, R.A., Moustafa, N.M and Faleh, N.M. (2020), "Finite element based modeling and thermal dynamic analysis of functionally graded graphene reinforced beams", *Adv. Comput. Design*, **5**(2), 177-193. https://doi.org/10.12989/acd.2020.5.2.177.

Avcar, M. (2019), "Free vibration of imperfect sigmoid and power law functionally graded beams", *Steel Compos. Struct.*, **30**(6), 603–615. https://doi.org/10.12989/scs.2019.30.6.603.

Baaskaran, N., Ponappa, K. and Shankar, S. (2018), "Assessment of dynamic crushing and energy absorption characteristics of thin-walled cylinders due to axial and oblique impact load", *Steel Compos. Struct.*, **28**(2), 179-194. https://doi.org/10.12989/scs.2018.28.2.179.

Batou, B., Nebab, M., Bennai, R., Atmane, H.A., Tounsi, A. and Bouremana, M. (2019), "Wave dispersion properties in imperfect sigmoid plates using various HSDTs", *Steel Compos. Struct.*, **33**(5), 699-716. https://doi.org/10.12989/scs.2019.33.5.699.

Chakrabarti, K.M. (1974)), "Note on Boundary layer in a dusty gas", *American Inst. Aeronautics and Astronautics J.*, **12**, 1136-1137. http://dx.doi.org/10.2514/3.49427.

Chen, J., Zhuang, Y., Fang, H., Liu, W., Zhu, L. and Fan, Z. (2019a), "Energy absorption of foam-filled lattice composite cylinders under lateral compressive loading", *Steel Compos. Struct.*, **31**(2), 133-148. https://doi.org/10.12989/scs.2019.31.2.133.

Chen, W., Ji, C., Alam, M.M. and Xu, D. (2019b), "Flow-induced vibrations of three circular cylinders in an equilateral triangular arrangement subjected to cross-flow", *Wind Struct.*, **29**(1), 43-53. https://doi.org/10.12989/was.2019.29.1.043.

Civalek, Ö. (2017), "Free vibration of carbon nanotubes reinforced (CNTR) and functionally graded shells and plates based on FSDT via discrete singular convolution method", *Compos. Part B: Eng.*, **111**, 45-59.

Derakhshandeh1a, J.F. and Alam, M.M. (2020), "Reynolds number effect on the flow past two tandem cylinders", *Wind Struct.*, **30**(5), 475-483. https://doi.org/10.12989/was.2020.30.5.475.

Iqbal, W., Naeem, M.N. and Jalil, M. (2019), "Numerical analysis of Williamson fluid flow along an exponentially stretching cylinder", *AIP Adv.*, **9**(5), 055118, http://dx.doi.org/10.1063/1.5092737.

Ishak, A. and Nazar, R. (2009), "Laminar boundary layer flow along a stretching cylinder", *Eur. J. Sci. Res.*, **36**(1), 22-29.

Ishak, A., Nazar, R. and Pop, I. (2008), "Uniform suction/ blowing effect on flow and heat transfer due to stretching cylinder", *App. Math. Mod.*, **32**, 2059-2066. http://dx.doi.org/10.1016/j.apm.2007.06.036.

Karami, B, Janghorban, M. and Tounsi, A. (2018), "Nonlocal strain gradient 3D elasticity theory for anisotropic spherical nanoparticles", *Steel Compos. Struct.*, **27**(2), 201-216. https://doi.org/10.12989/scs.2018.27.2.201.

Karami, B., Janghorban, M. and Tounsi, A. (2017), "Effects of triaxial magnetic field on the anisotropic nanoplates", *Steel Compos. Struct.*, **25**(3), 361-374. https://doi.org/10.12989/scs.2017.25.3.361.

Khan, M. and Malik, R. (2015), "Forced convective heat transfer to Sisko fluid flow past a stretching cylinder", *AIP Adv.*, **5**(12), 127202. http://dx.doi.org/10.1063/1.4937346.

Konch, J. and Hazarika, G.C. (2017), "Unsteady Hydro magnetic flow of dusty fluid over a stretching cylinder with variable viscosity and thermal conductivity", *Int. J. Adv. Sci. Tech.*, **99**, 57-70. http://dx.doi.org/10.14257/ijast.2017.99.05.

lmtiaz, M., Hayat, T. and Alsaedi, A. (2016), "Mixed convection flow of Casson nanofluid over a stretching cylinder with convective boundary conditions", *Adv. Power Tech.*, **27**(5), 2245-2256. https://doi.org/10.1016.j.apt.2016.08.011.

Loghman, A., Faegh, R.K. and Arefi, M. (2018), "Two dimensional time-dependent creep analysis of a thick-walled FG cylinder based on first order shear deformation theory", *Steel Compos. Struct.*, **26**(5), 533-547. https://doi.org/10.12989/scs.2018.26.5.533.

Madani, H., Hosseini, H. and Shokravi, M. (2016), "Differential cubature method for vibration analysis of embedded FG-CNT-reinforced piezoelectric cylindrical shells subjected to uniform and non-uniform temperature distributions", *Steel Compos. Struct.*, **22**(4), 889-913. https://doi.org/10.12989/scs.2016.22.4.889.

Mahdy, A. (2015), "Heat transfer and flow of a Casson fluid due to a stretching cylinder with the soret and dufour effects", *J. Eng. Phys. Thermophy.*, **88**(4), 928-936. https://doi.org/10.1007/s10891-015-1267-6.

Malik, M.Y., Hussain, A., Salahuddin, T., Awais, M., Bilal, S. and Khan, F. (2016), "Flow of Sisko fluid over a stretching cylinder and heat transfer with viscous dissipation and variable thermal conductivity: A numerical study", *AIP Adv.*, **6**(4), 045118. https://doi.org/10.1063/1.4948458.

Malik, M.Y., Naseer, M., Nadeem, S. and Rehman, A. (2013), "The boundary layer flow of Casson nanofluid over an exponentially stretching cylinder", *Appl. Nanosci.*, 4, 869-873. https://doi.org/10.1007/s 13204-013-0267-0.

Moghaddam, S.H. and Masoodi, A.R. (2019), "Elastoplastic nonlinear behavior of planar steel gabled frame", *Adv. Comput. Des.*, **4**(4), 397-413. https://doi.org/10.12989/acd.2019.4.4.397

Naseer, M., Malik, M.Y., Nadeem, S. and Rehman, A. (2014), "The boundary layer flow of hyperbolic tangent fluid over a vertical exponentially stretching cylinder", *Alexandria Eng. J.*, **53**, 747-750. https://doi.org/10.1016/j.aej.2014.05.001.

Rad, M.H.G., Shahabian, F. and Hosseini, S.M. (2020), "Geometrically nonlinear dynamic analysis of FG graphene platelets-reinforced nanocomposite cylinder: MLPG method based on a modified nonlinear micromechanical model", *Steel Compos. Struct.*, **35**(1), 77-92. https://doi.org/10.12989/scs.2020.35.1.077.

Rasekh, A., Ganji, D.D., Tavakoli, S., Ehsani, H. and Naeejee, S. (2014), "MHD flow and heat transfer of dusty fluid over a stretching hollow cylinder with a convective boundary conditions", *Heat Trans. Asian Res.*, **43**(3), 221-232. https://doi.org/10.1002/htj.21073.

Rebhi, A.D. (2010), "On boundary layer flow of dusty gas from a horizontal circular cylinder", *Braz. J. Chem. Eng.*, **27**(4), 653-662. http://dx.doi.org/10.1590/S0104-66322010000400017.

Rehman, A. (2015), "Boundary layer flow and heat transfer of Micropolar Fluid over a vertical exponentially stretching cylinder", *Appl. Comp. Math.*, 4(6), 424-430. http://dx.doi.org/10.11648/j.acm.20150406.15.

Saffman, P.G. (1962), "On the stability of laminar flow of a dusty gas", *J. Fluid Mech.*, **13**, 120-128. https://doi.org/10.1017/S0022112062000555.

Salah, F., Boucham, B., Bourada, F., Benzair, A., Bousahla, A.A. and Tounsi, A. (2019), "Investigation of thermal buckling properties of ceramic-metal FGM sandwich plates using 2D integral plate model", *Steel Compos. Struct.*, **33**(6), 805-822. https://doi.org/10.12989/scs.2019.33.6.805.

Salahuddin, T., Malik, M.Y., Hussain, A., Awais, M. and Bilal, S. (2017), "Mixed convection boundary layer flow of Williamson fluid with slip conditions over a stretching cylinder by using Keller-box method", *Int. J. Nonlinear Sci. Numer. Simul.*, **18**(1), 9-17. https://doi.org/10.1515/ijnsns.2015.0090.

Shadravan, S., Ramseyer, C.C. and Floyd, R.W. (2019), "Comparison of structural foam sheathing and oriented strand board panels of shear walls under lateral load", *Adv. Comput. Des.*, **4**(3), 251-272. https://doi.org/10.12989/acd.2019.4.3.251.

Sharma, N. and Panda, S.K. (2020a), "Multiphysical numerical (FE–BE) solution of sound radiation responses of laminated sandwich shell panel including curvature effect", *Comput. Math. Appl.*, **80**(5), 1221-1239.

Sharma, N., Mahapatra, T.R. and Panda, S.K. (2017a), "Vibro-acoustic behaviour of shear deformable laminated composite

flat panel using BEM and the higher order shear deformation theory", *Compos. Struct*., **180**, 116-129.
Sharma, N., Mahapatra, T. R. and Panda, S.K. (2017b), "Numerical study of vibro-acoustic responses of un-baffled multi-layered composite structure under various end conditions and experimental validation", *Latin Am. J. Solids Struct*., **14**(8), 1547-1568.
Sharma, N., Mahapatra, T.R. and Panda, S.K. (2017c), "Vibro-acoustic analysis of un-baffled curved composite panels with experimental validation", *Struct. Eng. Mech*., **64**(1), 93-107. https://doi.org/10.12989/sem.2017.64.1.093.
Sharma, N., Mahapatra, T.R. and Panda, S.K. (2018a), "Numerical analysis of acoustic radiation responses of shear deformable laminated composite shell panel in hygrothermal environment", *J. Sound Vib*., **431**, 346-366.
Sharma, N., Mahapatra, T.R. and Panda, S.K. (2018b), "Numerical analysis of acoustic radiation properties of laminated composite flat panel in thermal environment: a higher-order finite-boundary element approach", *Proceedings of the Institution of Mechanical Engineers Part C: J. Mech. Eng. Sci*., **232**(18), 3235-3249.
Sharma, N., Mahapatra, T.R. and Panda, S.K. (2018e), "Thermoacoustic behavior of laminated composite curved panels using higher-order finite-boundary element model", *Int. J. Appl. Mech*., **10**(2), 1850017.
Sharma, N., Mahapatra, T.R. and Panda, S.K. (2019a), "Hygrothermal effect on vibroacoustic behaviour of higher-order sandwich panel structure with laminated composite face sheets", *Eng. Struct*., **197**, 109355.
Sharma, N., Mahapatra, T.R. and Panda, S.K. (2019b), "Vibroacoustic analysis of thermo-elastic laminated composite sandwich curved panel: a higher-order FEM–BEM approach", *Int. J. Mech. Mater. Des*., **15**(2), 271-289
Sharma, N., Mahapatra, T.R., Panda, S.K. and Hirwani, C.K. (2018c), "Acoustic radiation and frequency response of higher-order shear deformable multilayered composite doubly curved shell panel–an experimental validation", *Appl. Acoustics*, **133**, 38-51.
Sharma, N., Mahapatra, T.R., Panda, S.K. and Katariya, P. (2020b), "Thermo-acoustic analysis of higher-order shear deformable laminated composite sandwich flat panel", *J. Sandw. Struct. Mater*., **22**(5), 1357-1385.
Sharma, N., Mahapatra, T.R., Panda, S.K. and Mehar, K. (2018d), "Evaluation of vibroacoustic responses of laminated composite sandwich structure using higher-order finite-boundary element model", *Steel Compos. Struct*., **28**(5), 629-639. https://doi.org/10.12989/scs.2018.28.5.629.
Simsek M. (2011), "Forced vibration of an embedded single-walled carbon nanotube traversed by a moving load using nonlocal Timoshenko beam theory", *Steel Compos. Struct*., **11**(1), 59-76. https://doi.org/10.12989/scs.2011.11.1.059.
Sofiyev, A.H., Yücel, K., Avcar, M. and Zerin, Z. (2006), "The dynamic stability of orthotropic cylindrical shells with non-homogenous material properties under axial compressive load varying as a parabolic function of time", *J. Reinforced Plastics Compos*., **25**(18), 1877-1886.
Wang, C.Y. (1988), "Fluid flow due to a stretching cylinder", *Phy. Fluids*, **31**, 466-468. https://doi.org/10.1063/1.866827.
Wang, C.Y. and Ng, C.O. (2011), "Slip flow due to a stretching cylinder", *Int. J. Non-Lin. Mech*., **46**, 1191-1194. https: //doi.org/10.1016/j.ijnonlinmec.2011.05.04.

CC